
Article:
Dixon Wilkins, M.C., Stennett, M.C. orcid.org/0000-0002-8363-9103 and Hyatt, N.C. (2019) The effect of A-site cation on the formation of brannerite (ATi2O6, A = U, Th, Ce) ceramic phases in a glass-ceramic composite system. MRS Advances, 5 (1-2). pp. 73-81. ISSN 2059-8521

https://doi.org/10.1557/adv.2019.470

MRS Advances

The Effect of A-Site Cation on the Formation of Brannerite (ATi_2O_6, A = U, Th, Ce) Ceramic Phases in a Glass-Ceramic Composite System

Malin C. Dixon Wilkins[1], Martin C. Stennett[1], and Neil C. Hyatt[1]

1 Immobilisation Science Laboratory, Department of Materials Science and Engineering, The University of Sheffield, Sheffield, UK

ABSTRACT

A range of stoichiometric and mixed A-site cation brannerite glass-ceramics have been synthesised and characterised. The formation of UTi_2O_6 in glass is reliant on ensuring all uranium remains tetravalent by processing in an inert atmosphere. $ThTi_2O_6$ forms in glass under both inert and oxidising atmospheres due to the lack of other easily available oxidation states. $CeTi_2O_6$ could not be made to form within this glass system. The formation of $A_{0.5}B_{0.5}Ti_2O_6$ phases depends strongly on the oxidation states of the A and B cations available in the process atmosphere, with the most successful compositions having an average final oxidation state of $(A,B)^{4+}$. Mixed cation brannerite compositions that formed in argon include $U_{0.75}Th_{0.25}Ti_2O_6$ and $U_{0.71}Ce_{0.29}Ti_2O_6$. Those forming in air include $U_{0.23}Th_{0.77}Ti_2O_6$, $Th_{0.37}Ce_{0.63}Ti_2O_6$, and $U_{0.41}Ce_{0.59}Ti_2O_6$.

INTRODUCTION

Brannerite (prototypically UTi_2O_6) is a naturally occurring titanate mineral phase containing a particularly high fraction of uranium (> 55% uranium by weight), and has been suggested as a possible candidate host for high actinide content wastes.[1] The analogous phase $ThTi_2O_6$ is relatively rare in nature,[2] but naturally occurring U-brannerites often have a high proportion of Th doped on the U site.[3,4] Natural samples of $CeTi_2O_6$ with the brannerite structure have not been observed.

It was first found that to successfully synthesise UTi_2O_6 the oxygen partial pressure in the sintering atmosphere must be minimised to retain all U as U^{4+}.[5,6] Mixed cation brannerite ceramics have previously been investigated, with the substitution of lower valent cations (Ca^{2+}, Y^{3+}, Gd^{3+}, and La^{3+}) stabilising the presence of higher valent U in the brannerite structure.[7–10] Brannerite ceramics have also been investigated as hosts

for MOX (mixed oxide, *i.e.* mixed UO_2 and PuO_2) fuels, $U_{0.9}Ce_{0.1}Ti_2O_6$ and $U_{0.81}Ce_{0.09}Gd_{0.1}Ti_2O_6$ (Ce as a surrogate for Pu) .[11]

A reasonable range of brannerite glass-ceramics have previously been reported in the literature, with the vast majority focussing on air-fired compositions following a batched ceramic stoichiometry of $U_{0.5}M_{0.5}Ti_2O_6$ (M is Tb^{3+}, Dy^{3+}, Y^{3+}, and Eu^{3+}).[12–14] Pu-containing glass-ceramics have also been synthesised ($Gd_{0.2}Pu_{0.5}U_{0.5}Ti_2O_6$ and $Gd_{0.1}Hf_{0.1}Pu_{0.2}U_{0.6}Ti_2O_6$),[13] which gives some indication that Pu is usefully soluble in UTi_2O_6, and does not interfere with the formation of these glass-ceramics. All of these glass-ceramics except one ($Gd_{0.1}Hf_{0.1}Pu_{0.2}U_{0.6}Ti_2O_6$) contained the same glass phase, $Na_2AlBSi_6O_{16}$, that has previously been demonstrated as a suitable glass for similar titanate-phase glass-ceramics.[15–17] $CeTi_2O_6$ glass-ceramics have also been investigated, however they were formed by simple co-sintering of pre-synthesised glass and ceramic phases.[18,19]

The synthesis of stoichiometric brannerite glass-ceramics has not been reported; this study examines the formation of the three stoichiometric titanate brannerites in $Na_2AlBSi_6O_{16}$ glass. In addition, glass-ceramics targeting the mixed cation phases $U_{0.5}Th_{0.5}Ti_2O_6$, $Th_{0.5}Ce_{0.5}Ti_2O_6$, and $Ce_{0.5}U_{0.5}Ti_2O_6$ were synthesised, to try and further elucidate the different behaviours of the cations studied within the brannerite structure.

In this investigation, brannerite glass-ceramics were synthesised by an all oxide solid-state route, in contrast to previous examples, which first made a ceramic precursor using an alkoxide/nitrate route that was then mixed with a glass precursor and heat-treated.

As noted in the literature, many ceramic brannerites seem to have some degree of non-stoichiometry, and it was expected that a certain amount of the TiO_2 would dissolve in the glass. As a result, samples were batched with a hyperstoichiometric amount of TiO_2. As-batched stoichiometry was $1AO_2 : 2.15TiO_2$. However, it was expected that any brannerite formed would closely follow the nominal ATi_2O_6 stoichiometry.

EXPERIMENTAL

Samples were prepared using a cold-press and sinter method. The targeted glass:ceramic ratio for all samples was 1:1 by weight. A glass precursor was prepared by calcining a homogenised mixture of SiO_2, H_3BO_3, $Na_2(CO_3)$, and Al_2O_3 at 600 °C for 6 hours. The ceramic precursors were then added as the component oxides (UO_2, ThO_2, CeO_2, TiO_2) and the mixture wet milled in isopropanol in a Fritsch Pulverisette 23 reciprocating ball mill for 5 minutes at 30 Hz. The resulting slurry was then dried in an oven at 85 °C, and the powder cakes retrieved and broken up using a mortar and pestle. The homogenised powders were pelletised under 2 t into 10 mm pellets. The pellets were then placed into crucibles lined with coarse ZrO_2 to prevent sticking, then heat treated (1200 °C, 12 hours, ramp rate of 5 $°Cmin^{-1}$) in a tube furnace under either argon or air. Any ZrO_2 adhered to the outside of the pellets was removed by hand.

The resulting pellets were then characterised. Pieces of the pellets were ground using a mortar and pestle, and powder x-ray diffraction (XRD) was used for phase identification (Bruker D2 Phaser, using Ni-filtered Cu K_α radiation). Diffraction patterns for refinement were collected on the same instrument, with LaB_6 used as a peak position standard.

Samples were prepared for Raman spectroscopy and scanning electron microscopy (SEM) by mounting in cold-set resin, before polishing to an optical finish. Raman spectra were collected from various points on the polished surface (Horiba XploRa PLUS Raman microscopy, 532 nm laser, 100x magnification). The samples were

carbon-coated to reduce sample charge build-up and SEM used to investigate the microstructure and phase assemblage, with energy-dispersive x-ray spectroscopy (EDX) being used to confirm the identities of phases observed (Hitachi TM3030, operating at 15 kV; Bruker Quantax 70 EDX system).

RESULTS AND DISCUSSION

UTi_2O_6 glass-ceramics

When heat-treated under argon, UTi_2O_6 was the majority phase formed, with some UO_2 and trace TiO_2 also observed in the XRD pattern (see Figure 1). The microstructure consists of uneven grains of UTi_2O_6 in the glass matrix. UO_2 is seen encapsulated in some grains of brannerite, as well as a small amount free in the glass. The Raman spectrum of the brannerite phase closely matches that of stoichiometric UTi_2O_6 as in reported in the literature.[20] Lattice parameters obtained from a Le Bail refinement (see Table 1) closely match those reported previously for stoichiometric UTi_2O_6.[21]

As expected from the related ceramic phase, UTi_2O_6 did not form in air[5,6] (see Figure 2). The main ceramic phases observed in the XRD pattern were U_3O_8 and rutile, indicating that all U was oxidised, thus preventing the brannerite structure from forming. The microstructure observed by SEM is in agreement with this, showing U_3O_8 and TiO_2 in a glassy matrix. A significant amount of uranium is dissolved in the glass, most likely as U^{5+} or U^{6+}; this occurs in all U-containing samples heated in air, and will be further discussed in later sections.

Table 1: Crystallographic details of brannerite phases produced in glass-ceramic composites, as determined by Le Bail refinements of XRD data and SEM-EDX.

Target composition		a (Å)	b (Å)	c (Å)	β (°)	V (Å^3)	EDX A-site composition
Ar	UTi_2O_6	9.8142(2)	3.7650(1)	6.9182(2)	118.913(2)	223.77	
	$U_{0.5}Th_{0.5}Ti_2O_6$	9.8174(5)	3.7818(2)	6.9592(3)	118.913(4)	226.17	$U_{0.75(3)}Th_{0.25(3)}$
	$ThTi_2O_6$	9.8125(3)	3.8224(1)	7.0329(2)	118.814(3)	231.12	
	$Ce_{0.5}U_{0.5}Ti_2O_6$	9.8165(3)	3.7615(1)	6.9580(2)	118.659(3)	225.44	$U_{0.71(3)}Ce_{0.29(3)}$
Air	$U_{0.5}Th_{0.5}Ti_2O_6$	9.8150(7)	3.7857(2)	6.9803(5)	118.745(6)	227.40	$U_{0.23(1)}Th_{0.77(1)}$
	$ThTi_2O_6$	9.8123(3)	3.8223(1)	7.0326(2)	118.810(2)	231.11	
	$Th_{0.5}Ce_{0.5}Ti_2O_6$	9.8204(5)	3.7732(2)	6.9393(4)	119.041(4)	224.80	$Th_{0.37(2)}Ce_{0.63(2)}$
	$Ce_{0.5}U_{0.5}Ti_2O_6$	9.8101(3)	3.7496(1)	6.9517(2)	118.564(2)	224.59	$U_{0.41(3)}Ce_{0.59(3)}$

$ThTi_2O_6$ glass-ceramics

The phase assemblage of the produced $ThTi_2O_6$ glass-ceramics was unchanged with respect to processing atmosphere. The XRD patterns of both samples consist of brannerite, $ThTi_2O_6$, and unreacted component oxides, ThO_2 and TiO_2. The microstructures observed by SEM were in good agreement, comprising large regions of ThO_2 encapsulated by brannerite and smaller grains of TiO_2 held within the glassy matrix (see Figure 3). The large amount of unreacted material is likely due to the refractory nature of ThO_2 (ceramic $ThTi_2O_6$ usually requires temperatures of 1400 °C or above to form).[22,23]

Both the observed Raman spectra and the lattice parameters determined from a Le Bail refinement closely match those reported in the literature for stoichiometric $ThTi_2O_6$.

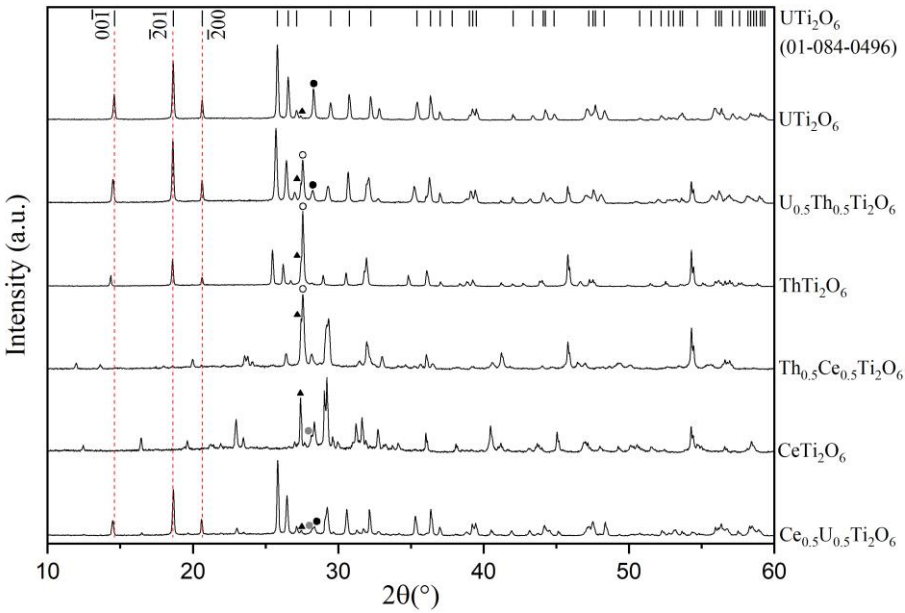

Figure 1: Diffraction patterns of glass-ceramic composites heat-treated under argon. Each pattern is labelled with the as-batched target ceramic composition. The peak positions of stoichiometric UTi_2O_6 are shown by the tick marks above, the positions of the first three peaks are also indicated by dashed red lines. Black circles represent the major peaks of UO_2; white, ThO_2; grey, CeO_2; black triangles, TiO_2.

$CeTi_2O_6$ glass-ceramics

In contrast to the compositions targeting $ThTi_2O_6$, $CeTi_2O_6$ did not form in argon on air. The produced phase assemblages differed depending on the oxidation state of cerium over the course of the reaction. It is well-established that the Ce^{3+}/Ce^{4+} redox couple is strongly temperature dependent, with cerium oxides self-reducing at high temperatures.

When heated under argon, Ce^{3+} forms, releasing O_2 that is then lost in the flowing gas, and the material cannot re-oxidise to Ce^{4+} on cooling as a result. Because of this, the only Ce-containing crystalline phases observed by XRD and SEM are exclusively Ce^{3+} species, including $Ce_2Ti_2SiO_9$ (Ce-trimounsite) and $Ce_2Ti_2O_7$ (a large amount of TiO_2 is also observed).

When heated in air, the phases in the final glass-ceramic product are CeO_2 and TiO_2. There are two possible reasons for the presence of Ce^{4+} but lack of brannerite. The presence of Ce^{3+} at temperature may prevent formation of brannerite, and during cooling the material re-oxidises forming CeO_2. Or, the increased partial pressure of O_2 in the atmosphere may be sufficient to make the auto-reduction to Ce^{3+} unfavourable, and there is a different factor preventing formation of $CeTi_2O_6$. At this point, it is unclear which is the dominant mechanism.

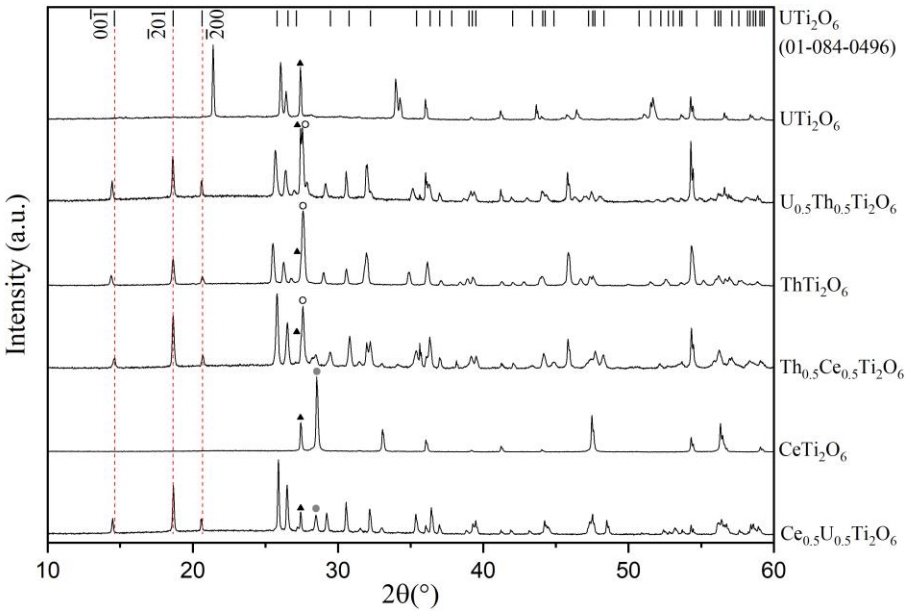

Figure 2: Diffraction patterns of glass-ceramic composites heat-treated in air. Each pattern is labelled with the as-batched target ceramic composition. The peak positions of stoichiometric UTi_2O_6 are shown by the tick marks above, the positions of the first three peaks are also indicated by dashed red lines. Black circles represent the major peaks of UO_2; white, ThO_2; grey, CeO_2; black triangles, TiO_2.

$U_{0.5}Th_{0.5}Ti_2O_6$ glass-ceramics

The sample heated under argon produced phases consistent with the U- and Th-endmembers. The XRD pattern confirms the presence of brannerite as the majority ceramic phase, with ThO_2 and smaller amounts of UO_2 and TiO_2. The microstructure observed by SEM was consistent with the Th- and U-endmembers, with brannerite forming the major phase accompanied by grains of UO_2 (encapsulated in brannerite) and TiO_2 (held in the glass matrix), and larger clusters of ThO_2 (see Figure 3). The relative amount of unreacted AnO_2 (where An = U, Th) was approximately less than that seen in the sample targeting $ThTi_2O_6$, but more than the UTi_2O_6 endmember.

The lattice parameters were determined by a Le Bail fit, with the b and c lattice parameters being slightly larger than those of the UTi_2O_6 endmember, but smaller than those of the $ThTi_2O_6$ endmember. Considering the relative magnitude of the lattice parameters qualitatively, it appears that the average ion size of the $(U,Th)Ti_2O_6$ composition is closer to that of UTi_2O_6 than $ThTi_2O_6$. EDX was used to determine the U:Th ratio in the brannerite phase, giving an overall observed stoichiometry of $U_{0.75}Th_{0.25}Ti_2O_6$ (assuming Ti and O follow the nominal stoichiometry), in good agreement with the observed lattice parameters.

As observed by XRD, the sample heated under air had a similar phase assemblage as the sample heated under argon, with the exception of a larger amount of unreacted ThO_2 and TiO_2. The microstructure observed by SEM was also similar, consisting of grains of brannerite, some of which are encapsulating large grains of ThO_2, and smaller regions of TiO_2. The determined lattice parameters were notably larger, suggesting a higher Th content than for the Ar-fired counterpart. This was confirmed by EDX giving an overall observed stoichiometry of $U_{0.23}Th_{0.77}Ti_2O_6$ (assuming Ti and O follow the nominal stoichiometry). The remainder of the uranium appears to be dissolved

in the glass, with the glass composition as determined by EDX showing approximately ten times the amount of uranium when compared to the sample fired in argon; this suggests that a significant proportion of the uranium was oxidised to U^{5+} and/or U^{6+} during processing (it is well-established that U^{5+} and U^{6+} are more soluble in alumino- and borosilicate glasses).[24,25] It is not clear if the brannerite-forming uranium is U^{4+} or has been oxidised, with either A-site or oxygen vacancies to charge balance.

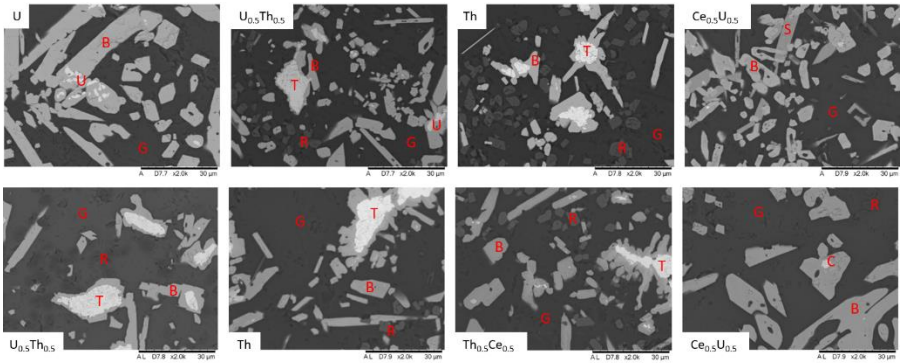

Figure 3: Representative SEM micrographs of the microstructures of all samples that formed brannerite-structured ceramic phases. The top row are those fired under argon, the bottom row are those fired in air. Each micrograph is labelled by the as-batched A-site stoichiometry. B is brannerite, U is UO_2, T is ThO_2, C is CeO_2, R is TiO_2, S is $Ce_2Ti_2SiO_9$, and G is glass.

$Th_{0.5}Ce_{0.5}Ti_2O_6$ glass-ceramics

When processed in argon, no brannerite formed; however, several different phases were observed by XRD, including unreacted ThO_2 and TiO_2, and various Ce^{3+} phases, possibly including $Ce_2Ti_2SiO_9$, as seen in the $CeTi_2O_6$ endmember when heated in argon. Although the lack of cerium-containing brannerite phases was expected, it is unclear why no $ThTi_2O_6$ was observed, when it formed reasonably well in the Th-endmember under both neutral and oxidising atmospheres.

When processed in air, brannerite was the major phase formed, with ThO_2 and TiO_2, and trace amounts of CeO_2. The stoichiometry of the ceramic phase was determined by EDX to be $Th_{0.37}Ce_{0.63}Ti_2O_6$, as expected from the large amount of ThO_2 remaining unreacted. Although Ce^{3+} has been observed in U^{5+} air-fired brannerites before[11,14] due to the lack of higher oxidation states of thorium, it is reasonable to assume that all cerium and thorium is present as Ce^{4+} and Th^{4+} respectively, giving an average A-site ionic radius of 0.89604 Å. With this assumption in mind, the lattice parameters determined from a Le Bail refinement follow the general trend seen in brannerites, where an increase in A-site ion size causes a related increase in the b and c lattice parameters, as well as unit cell volume (see Figure 4).

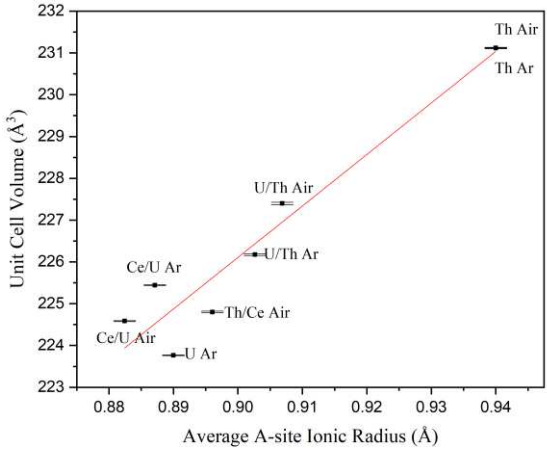

Figure 4: Plot of average A-site ionic radii (as determined from EDX stoichiometries) against unit cell volume as determined by Le Bail refinements. Each point is labelled according to the cations present. The trend line indicated has an R^2 value of 0.9405. The standard errors associated with the refinement models are also indicated.

$Ce_{0.5}U_{0.5}Ti_2O_6$ glass-ceramics

A glass-ceramic targeting a ceramic composition $Ce^{3+}{}_{0.5}U^{5+}{}_{0.5}Ti_2O_6$ has previously been reported, using an alkoxide/nitrate route starting from trivalent cerium nitrate and processing in air[14]. It was noted that the final produced ceramic phase $Ce_{0.65}U_{0.35}Ti_2O_6$ was U-deficient compared to the target stoichiometry due to mixed cerium valence, with the remaining uranium being dissolved in the glass phase.

When processed in argon, the major phase observed by XRD was brannerite, with minor amounts of UO_2 and $Ce_2Ti_2SiO_9$, and trace rutile, as expected from the behaviour of the two endmembers in argon. The stoichiometry of the brannerite phase was determined by EDX to be $U_{0.71}Ce_{0.29}Ti_2O_6$.

Preliminary XANES measurements of the Ce and U oxidation states suggest A-site oxidation states of $Ce^{3+}/U^{4,5+}$, where the inclusion of each Ce^{3+} is charge balanced by the oxidation of U^{4+} to U^{5+}. The average A-site ionic radius in this case is 0.887 Å, which closely follows the trend in the effect of ion size on unit cell volume (see Figure 4).

When processed in air, the phase assemblage was broadly similar to that reported in the literature: brannerite as the major phase, with lesser amounts of TiO_2 and a cubic mixed oxide, $(Ce,U)O_2$. The stoichiometry of the brannerite phase was determined by EDX to be $U_{0.41}Ce_{0.59}Ti_2O_6$, slightly enriched in uranium compared to the $U_{0.35}Ce_{0.65}Ti_2O_6$ described in the literature, but likely following the same trend of U^{5+} with mixed Ce^{3+}/Ce^{4+}. As seen in the other uranium bearing samples heated in air, a considerable amount of uranium is dissolved in the glass (approximately nine times the amount of the argon fired sample as determined by EDX), due to the increased solubility of higher valent uranium previously mentioned. This accounts for the excess oxidised uranium that did not form brannerite due to the higher Ce content.

The unit cell parameters as determined by the Le Bail method are within the expected range (and closely match those reported for $Ce_{0.65}U_{0.35}Ti_2O_6$), but cannot be directly compared to a wider range of brannerites without making assumed assignments of the oxidation states of uranium and cerium. The most likely assignment is that of sufficient Ce^{3+} to charge balance all uranium as U^{5+}, with the remainder of the cerium

tetravalent. If this is the case, the average A-site ion size would be 0.882 Å, which is in good agreement with the general trend (see Figure 4).

CONCLUSION

As expected from previous literature reports of uranium-containing brannerites, the most important factor in producing a targeted brannerite phase as the ceramic component in these glass-ceramic systems appears to be retaining an average oxidation state of the A-site cations of 4+. As a result, $ThTi_2O_6$ is insensitive to different atmospheres during processing, but does not form at a high yield over these timescales (this is most likely due to the refractory nature of ThO_2 rather than any thermodynamic effect). UTi_2O_6 only forms in argon, and $CeTi_2O_6$ did not form at all, due to auto-reduction of cerium at temperature.

Of the mixed cation compositions, $U_{0.5}Ce_{0.5}Ti_2O_6$ formed high yields of brannerite both in air, as a $Ce^{3,4+}/U^{5+}$ system, and in argon, presumably as a $Ce^{3+}/U^{4,5+}$ brannerite as determined from the lattice parameters and preliminary XANES measurements. The differences in solubility of cerium appears to depend strongly on what charge balancing mechanisms exist. The solid solubility between UTi_2O_6 and $ThTi_2O_6$ in these glass-ceramic systems seems high; however, the large amount of unreacted oxides suggests longer heat treatments are necessary to reach equilibrium (especially due to the refractory nature of ThO_2).

As reported in the literature, the unit cell parameters (especially b and c, as previously reported for other brannerites), as well as the unit cell volume, have a close correlation to the average A-site ion size. This effect most obvious for the argon fired series UTi_2O_6, $U_{0.75}Th_{0.25}Ti_2O_6$, $ThTi_2O_6$, as no non-tetravalent oxidation states are observed in these samples.

ACKNOWLEDGEMENTS

MDW is thankful to the UK EPSRC and Nuclear Decommissioning Authority for providing studentship through an EPSRC iCASE award. This work was performed in part in the MIDAS facility at The University of Sheffield, which was established with support from the Department for Energy and Climate Change, now incorporated within the Department for Business, Energy and Industrial Strategy. NCH is grateful to the Royal Academy of Engineering and the Nuclear Decommissioning Authority for funding.

Reference

1. E.R. Vance, M.L. Carter, G.R. Lumpkin, R.A. Day, and B.D. Begg, *Solid Solubilities of Pu, U, Gd and Hf in Candidate Ceramic Nuclear Wasteforms* (Australian Nuclear Science and Technology Organization, Menai, NSW 2234, Australia (US), 2001).
2. Y.D. Gotman and I.A. Khapaev, Zap Vses Miner. Obshch **87**, 201 (1958).
3. G.R. Lumpkin, S.H.F. Leung, and J. Ferenczy, Chem. Geol. **291**, 55 (2012).
4. F.A. Charalambous, R. Ram, M.I. Pownceby, J. Tardio, and S.K. Bhargava, Miner. Eng. **39**, 276 (2012).
5. J.E. Patchett and E.W. Nuffield, Can. Minerol. **6**, 483 (1960).
6. S. Kaiman, Can. Mineral. **6**, 389 (1959).
7. E.R. Vance, J.N. Watson, M.L. Carter, R.A. Day, and B.D. Begg, J. Am. Ceram. Soc. **84**, 141 (2001).
8. M. James and J.N. Watson, J. Solid State Chem. **165**, 261 (2002).
9. M. James, M.L. Carter, and J.N. Watson, J. Solid State Chem. **174**, 329 (2003).

10. D.J. Bailey, M.C. Stennett, and N.C. Hyatt, Procedia Chem. **21**, 371 (2016).
11. D.J. Bailey, M.C. Stennett, and N.C. Hyatt, MRS Adv. **2**, 557 (2017).
12. Y. Zhang, T. Wei, Z. Zhang, L. Kong, P. Dayal, and D.J. Gregg, J. Am. Ceram. Soc. **102**, 7699 (2019).
13. Y. Zhang, L. Kong, I. Karatchevtseva, R.D. Aughterson, D.J. Gregg, and G. Triani, J. Am. Ceram. Soc. **100**, 4341 (2017).
14. Y. Zhang, I. Karatchevtseva, L. Kong, T. Wei, and Z. Zhang, J. Am. Ceram. Soc. **101**, 5219 (2018).
15. Y. Zhang, L. Kong, R.D. Aughterson, I. Karatchevtseva, and R. Zheng, J. Am. Ceram. Soc. **100**, 5335 (2017).
16. L. Kong, I. Karatchevtseva, and Y. Zhang, J. Eur. Ceram. Soc. **37**, 4963 (2017).
17. E. Maddrell, S. Thornber, and N.C. Hyatt, J. Nucl. Mater. **456**, 461 (2015).
18. E. Paknahad and A.P. Grosvenor, Solid State Sci. **74**, 109 (2017).
19. E. Paknahad and A.P. Grosvenor, Can. J. Chem. **95**, 1110 (2017).
20. Y. Zhang, I. Karatchevtseva, M. Qin, S.C. Middleburgh, and G.R. Lumpkin, J. Nucl. Mater. **437**, 149 (2013).
21. J.T. Szymanski and J.D. Scott, Can. Mineral. **20**, 271 (1982).
22. K.S. Finnie, Z. Zhang, E.R. Vance, and M.L. Carter, J. Nucl. Mater. **317**, 46 (2003).
23. Y. Zhang, D.J. Gregg, G.R. Lumpkin, B.D. Begg, and M. Jovanovic, J. Alloys Compd. **581**, 665 (2013).
24. H. Schreiber and G. Balazs, Phys. Chem. Glas. **23**, 139 (1982).
25. H. Schreiber, G. Balazs, P. Jamison, and A. Shaffer, Phys. Chem. Glas. **23**, 147 (1982).